

1 **Astrobiology**

2

3

4

5

6 Fluctuation Analysis of Redox Potential to Distinguish Microbial Fe(II) Oxidation

7 A.M.L. Enright* and F.G. Ferris

8 Department of Earth Sciences

9 University of Toronto

10 Toronto, ON

11 M5S 3B1

12 CANADA

13 Corresponding author: enright@es.utoronto.ca

14 Running Title: Fluctuation Analysis of Redox Potential

15

16 **Abstract**

17 We developed a novel method for distinguishing abiotic and biological iron oxidation
18 in liquid media using oxidation-reduction (redox) potential time series data. The
19 instrument and processing algorithm were tested by immersing the tip of a Pt
20 electrode with an Ag-AgCl reference electrode, into an active iron-oxidizing biofilm
21 in a groundwater discharge zone, as well as in two abiotic systems: a killed sample
22 and a chemical control from the same site. We used detrended fluctuation analysis
23 to characterize average root-mean-square fluctuation behaviour, which was distinct
24 in the live system. The calculated α value scaling exponents determined by
25 detrended fluctuation analysis were significantly different at $p < 0.001$. This
26 indicates that time series of electrode response data may be used to distinguish live
27 and abiotic chemical reaction pathways. Due to the simplicity, portability, and small
28 size, it may be suitable for characterization of extraterrestrial environments where
29 water has been observed, such as Mars and Europa.

30

31

32 Keywords: oxidation-reduction potential, detrended fluctuation analysis, iron-
33 oxidizing bacteria

34

35

36

37

38

39

40

41

42

43

44

45

46

47

48

49

50

51

52

53

54

55

56

57

58

59 **1. Introduction**

60

61 Measurement of oxidation-reduction (redox) potential is one of the most elementary
62 and fundamental aspects of characterizing microbial niches. Redox potentials are
63 measured in many environmental systems to assess the type and role of biological
64 activity (Bohn, 1971). *In situ*, continuous measurement of redox potential has been
65 used to infer changes in microbial community dynamics and shifts in physiological
66 processes (van Bochove *et al.*, 2002), including shifts from aerobic to anaerobic
67 respiration.

68 The redox state of any aqueous environment is the quotient of the chemical activity
69 of dissolved oxidized and reduced chemical species, as shown in the Nernst
70 equation:

71
$$E = E^0 + \frac{RT}{nF} \ln Q$$

72 where E is the electrochemical potential of the cell, R is the universal gas constant,
73 T is absolute temperature, n is the number of electrons participating per atom, F is
74 Faraday's constant, and Q is the reaction quotient, $\frac{[\text{oxidized species}]}{[\text{reduced species}]}$. Redox potential is
75 sensitive even to subtle changes in chemical speciation. Environmental factors
76 including temperature, pH, and the presence of multiple redox couples, as well as
77 microbe-specific factors such as nutrient levels, solution chemistry, and oxygen
78 availability, can influence the redox potential of a microbial system (Newman and
79 Banfield, 2002).

80 Microbial metabolic reactions transfer electrons from a reduced donor species and
81 to an oxidized terminal electron acceptor, harnessing the energy released for cellular
82 functions (Weber *et al.*, 2006). As such, microbial bioenergetic metabolic activity is
83 based on redox reactions; additionally, other metabolic reactions such as
84 fermentation reactions can produce and consume redox active species. In this way,
85 all metabolically active microorganisms directly influence the relative abundance of
86 redox active substances, and chemical properties of their environment (van Bochove
87 *et al.*, 2002; Bethke *et al.*, 2011). Microbes mediate redox reactions which can cause
88 significant changes in pH and redox potential. Since redox potential represents a
89 physically constrained measurement of a biological system, the biological

90 manipulation of redox potential creates an opportunity to directly examine microbial
91 influence on physicochemical system parameters.

92 Characterizing *in situ* microbial activity remains a pressing issue in environmental
93 microbiology as 99% of microorganisms cannot be cultured (Hugenholtz *et al.*, 1998).
94 At present, describing microbial activity in pristine and contaminated environments
95 most often involves measurement of specific metabolite concentrations in samples
96 recovered from study sites of interest as well as studies using –omics approaches to
97 determine community metabolic potential (genomics), gene expression
98 (transcriptomics), and protein profiles (proteomics) (Dick and Lam, 2015). A
99 technique which could distinguish between microbial and abiotic processes
100 passively, *in situ*, would be an incredibly useful complement that could guide
101 microbiological sampling and study, but monitor systems on a longer term basis.
102 Here we present a novel method of analyzing *in situ* bacterial activity by the
103 correlation strength of time series of redox potential in a series of circumneutral,
104 microaerophilic, Fe(II)-oxidizing systems. We have analyzed three chemically similar
105 solutions from the same source – one live, and two abiotic (mimicking autocatalytic
106 and homogenous oxidation, respectively) (Melton *et al.*, 2014) – to determine the
107 sensitivity of electrode response time series to changes in electrode response
108 induced by the presence of microbes. We hypothesize that these differences in
109 correlation strength arise from biological activity wherein cell surfaces not only act
110 as reactive substrates, but where microbes also actively manipulate the movement
111 of O₂, Fe₂₊ and Fe₃₊, their metabolic substrates and products, giving rise to
112 correlation.

113 This technique does not rely on constraining environmental or physiochemical
114 conditions of a niche; instead, it depends on the diffusion of metabolically-
115 significant, redox active species in solution (Oldham, 1966; Frateur *et al.*, 1999;
116 Mampallil *et al.*, 2013). The method uses low cost, straightforward instrumentation,
117 allows broad comparisons between diverse systems, and does not necessitate
118 either removing organisms from their niches or collecting samples of biomass for
119 genomic analysis; all data is collected passively *in situ*. Any niche accessible to an
120 electrode is suitable for this type of analysis.

121 Fluctuations of electrode response arise from the motion of dissolved chemical
122 species, also known as Brownian motion or diffusion (Gabrielli *et al.*, 1993; Eliazar
123 and Shlesinger, 2013). Correlation is a property of a time series or process that
124 describes the statistical dependence of directly and distantly neighbored values
125 (Witt and Malamud, 2013); long-range correlations are where all or almost all values
126 are correlated with one another, that is, values are correlated with one another at
127 very long lags in time (Taqqu and Samorodnitsky, 1992; Beran 1994; Witt and
128 Malamud, 2013). Detrended fluctuation analysis (DFA) calculates a relationship
129 between root mean-square (RMS) fluctuation and time by quantifying the strength
130 of long range correlation in a time series (Hardstone *et al.*, 2012; Witt and Malamud,
131 2013).

132 Here, detrended fluctuation analysis is used to assess time-domain, self-similarity
133 and correlation behaviour in biological and chemical systems. We hypothesize that
134 statistically significant differences in fluctuation patterns of redox potential, as
135 evidenced by differences in scaling exponents, are the result of biological influence
136 on redox transformations, or, in the case of chemical systems, the lack of biological
137 activity. We suggest that measuring the redox potential time series could be a good
138 complement to the analysis of metabolites and genetic sequences, i.e., multiple
139 measurements of several different system parameters.

140 Iron-oxidizing systems are well suited for this type of analysis because of the direct
141 link between iron redox state to both cellular metabolism and the redox potential of
142 a solution, with a concomitant voltage change. Organisms that exploit the
143 Fe(III)/Fe(II) redox couple to fuel cellular growth underpin global biogeochemical
144 cycling of iron (Weber *et al.*, 2006; Emerson *et al.*, 2010).

145 In addition to varied terrestrial systems, this method may specifically be relevant to
146 future missions to Mars (Bibring *et al.*, 2004), Europa (Kargel *et al.*, 2000), Enceladus
147 (Waite *et al.*, 2009), or other environments where liquid, and especially water, is
148 known to be present. Redox instability has been documented on the surface of Mars
149 (McSween Jr. *et al.*, 1999), implying that given suitable geochemical conditions, Fe-
150 based biological activity might be possible.

151 **2. Methods**

152 **2.1 Instrumentation**

154

155 Electrode response time series were collected using a NI6009-USB data acquisition
156 device (DAQ) interfaced with a PC running LabVIEW using standard National
157 Instruments DAQmx VIs. This set up is intended for measuring voltage time-series
158 in aqueous environments with a design that: (1) allows portability for use in the
159 field, (2) is straightforward for interfacing and programming, and (3) provides a cost-
160 effective tool for accurate and reproducible measurements. Figure 1 describes the
161 experimental set-up. The DAQ was configured to measure voltage from the
162 electrode in analog mode using differential inputs, where the Pt wire was ground-
163 referenced to a heavy iron rod driven at least 18 cm into soil, located a minimum of 2
164 m from the point of sampling in a hydrologically separated area. This reference
165 location is typically in an unsaturated zone above and away from the measured
166 environment. The DAQ was placed inside a metal box which was fitted with a BNC
167 feedthrough to connect the differential inputs of the DAQ to the BNC signal cable
168 from the electrode and a USB outlet for connecting the DAQ to the PC. The
169 shielding of the electrode BNC signal cable, the DAQ ground, and the ground of
170 the PC were all connected to the heavy iron grounding rod. This strategy was found
171 to eliminate pickup noise.

172 By measuring the potential across the electrode in differential mode, any further
173 variations in common mode noise were eliminated. Additional testing to assess the
174 impact of aliasing was achieved using a Tektronix TDS 3054B oscilloscope, and
175 testing indicated no visible contributions from common noise sources. No anti-
176 aliasing filters were applied, because specifying a low-pass band assumes *a priori*
177 knowledge of the frequency range where chemical reactions contributing to
178 fluctuations would be observed.

179 Measurements are performed by immersing the tip of a double-junction, gel-filled
180 redox electrode (combination Pt Ag/Ag-Cl) in the aqueous medium for sampling.
181 Measurements were collected at a sampling frequency of 500 Hz for approximately
182 12 minutes, then downsampled to individual realizations of 2-10 Hz. Oversampling
183 was intentionally performed to permit statistical analysis on a pool of estimates,
184 without having to make initial assumptions about scaling range or chemical
185 interactions which might contribute to scaling.

186 Once immersed, redox-active ions in solution become mobile across a ceramic plug
187 in the tip of the electrode due to the difference in electrochemical potential between
188 the Pt tip and a reference Ag wire immersed in a KCl gel. The selection of Pt
189 electrodes was based on the extensive use of Pt electrodes in environmental
190 electrochemical studies (Fluhler *et al.*, 1976; Faulkner *et al.*, 1989; Vershinin and
191 Rozanov, 1993; Swerhone *et al.*, 1999; Sampedro *et al.*, 1999; van Bochove *et al.*, 2002;
192 Kasem and Jones, 2008; Ojumu *et al.*, 2008), often for measuring redox potential and
193 dissolved oxygen (Whitfield, 1969; Swerhone *et al.*, 1999). Pt electrodes have been
194 used continuously for measurements recorded over years, with either no or minimal
195 changes in performance over the time scale of the study (Smith *et al.*, 1978; Austin
196 and Huddleston, 1999; Swerhone *et al.*, 1999; van Bochove, 2002), and are known to
197 be reliable under a variety of environmental conditions (Kasem and Jones, 2008).
198 Additionally, as this test system is characterized by circumneutral, microaerophilic
199 Fe(II) - oxidation, we have selected an electrode assuming that the electrode
200 selected is responsive to the diffusing species of interest; Pt electrodes are known
201 to be sensitive to the metabolic species of interest, dissolved Fe(II), as long as
202 concentrations are higher than 10^{-5} M (Vershinin and Rozanov, 1993; Stumm and
203 Morgan, 1996), which they are for this site (James and Ferris, 2004; Ferris *et al.*,
204 2016).

205 When describing electrode response in diffusion-limited systems, both theoretical
206 and laboratory studies have indicated that current is influenced by the redox state of
207 the species in bulk solution, and not by the electrode making the measurements
208 (Mampallil *et al.*, 2013); this is important as it confirms that redox potential and
209 fluctuations being measured arise from the dynamics of the system as a whole, and
210 not from the microenvironment immediately surrounding the electrode tip.

211

212 *2.2 Processing Method*

213 Collected time series were analyzed in MatLAB using a custom detrended
214 fluctuation analysis (DFA) routine (Peng *et al.*, 1994). Shuffled data sets were
215 created by shuffling the time series index using the “rand” function approximately
216 50-100 times before processing.

217 The first step in DFA data processing is to remove the mean and integrate the time
218 series. The time series is divided into windows of length n . A least squares fit is
219 calculated for each window, and the integrated signal is detrended by subtracting
220 the local trend. The average fluctuation per window is calculated using a root mean
221 square (RMS) algorithm, and the value for the average fluctuation, $F(n)$, is plotted
222 against the window-size, n , in log space. If a straight line is observed over a range of
223 time windows, the time-series is persistent within that range, thus defining a scaling
224 range. The slope of this line is the α value, or scaling exponent. Finally, the
225 magnitude of α provides information about the strength of the long-range
226 correlation behavior of the time series (Hardstone *et al.*, 2012). Brownian motion
227 gives rise to a scaling exponent $\alpha = 1$ (Metzler and Klafter, 2000; Ramanujan *et al.*,
228 2006); with $1 < \alpha < 2$ relating to processes exhibiting fractional Brownian motion
229 (Metzler and Klafter, 2000; Eliazar and Shlesinger, 2013).

230 In random uncorrelated time series, such as Gaussian white noise $\alpha = 0.5$ (Metzler
231 and Klafter, 2000; Witt and Malamud, 2013), while $\alpha < 0.5$ indicates negative
232 persistence and $\alpha > 0.5$ indicates positive persistence (Peng *et al.*, 1994; Peng *et al.*,
233 1995; Metzler and Klafter, 2000; Hardstone *et al.*, 2012; Witt and Malamud, 2013).

234 DFA provides two significant advantages over the more common Fourier analysis: no
235 assumption of linearity, stationarity or independence of measurements is made, and
236 the amount of time required for a complete data set is achieved at $n = \sim 10^3$,
237 regardless of the sampling frequency (Metzler and Klafter, 2000; Shao *et al.*, 2012).

238 The inherent variability of field conditions over hours and days creates a preference
239 for shorter time series, where stable conditions over the measurement window could
240 be reasonably expected. However, the minimum time series length must be long
241 enough in real time to cover the entire scaling range.

242 Collection of very long (several hours) low-frequency time series is complicated in
243 field settings due to changes in conditions, such as temperature and light, over the
244 course of a day. Environmental time series analyses are also complicated by the
245 complexity of the chemical interactions being studied, the slower time scales of
246 kinetic processes that give rise to fluctuations, and inherent variability of dilute
247 aqueous systems. While several other time domain techniques are available, such

248 as fluctuation analysis, adaptive fractal analysis, (Riley *et al.*, 2012), and detrended
249 moving average analysis, DFA consistently performs well while requiring
250 time series of only $n=1000$ measurements (Shao *et al.*, 2012).

251

252 2.3 Field Site

253 In order to specifically isolate the biological influence on fluctuations, a well
254 characterized test site which hosts a thriving circumneutral microaerophilic Fe(II)-
255 oxidizing microbial mat was used to test the field-suitability of the technique. The
256 study site has been described in detail by James and Ferris (2004). Briefly, it is an
257 anoxic anaerobic iron-rich groundwater seep colonized by a thriving microbial mat
258 produced by *Leptothrix ochracea* with a minor component of *Gallionella ferruginea*
259 (James and Ferris, 2004). Oxygen for the oxidation of Fe(II) is supplied from the
260 atmosphere, and the seep intersects a fully aerated stream about 3 m from the seep
261 source; the reduced, anoxic groundwater is spatially confined to the narrow, shallow
262 (3-15 cm) creek.

263 In addition to an *in situ* sample, two controls were prepared: a killed sample was
264 used to evaluate the influence of the flocculent bacteriogenic iron oxides (BIOS)
265 that are precipitated by the Fe(II)-oxidizing microbial community (autocatalytic
266 oxidation; Melton *et al.*, 2014), and a chemical control which removed both biological
267 activity and the flocculent iron oxide particles (homogenous oxidation; Melton *et al.*,
268 2014). The killed sample was prepared by collecting an aliquot of BIOS of equal
269 volume to the Live system microcosm (described below), and sterilizing it by
270 autoclaving. The chemical control was prepared by filtering water from the extant
271 biofilm with 0.22 μm syringe filters. Microcosms were prepared and measured creek-
272 side, with the time elapsing between removing the water from the creek and the first
273 measurement at less than five minutes.

274

275 2.4 Determining Fe(II) Oxidation Rate Constants

276 Pseudo-first order oxidation rate constants were determined for the live system and
277 both controls to confirm that the extant biofilm was active at the time of
278 measurement. The protocol used for the microcosms was described by Ferris *et al.*
279 (2016). Measurements of dissolved Fe_{2+} and total Fe were collected every 30
280 minutes for 2 hours.

281 2.5 Additional Test Solutions

282 To create a test scenario as close as possible to an equilibrium state, the electrode
283 was allowed to rest in an aluminum foil-wrapped bottle of 3 M KCl solution for
284 several weeks, after which a time series was collected.

285 3. Results

286 3.1 Oxidation Rate Constants

287 The pseudo-first order oxidation rate constants were determined to be 0.0093
288 minute⁻¹ for the live sample, 0.0069 minute⁻¹ for the autoclaved sample, and 0.0019
289 minute⁻¹ for a filtered creek water sample; broadly consistent with the results
290 reported by James and Ferris (2004) and Ferris *et al.* (2016) for the same site. The
291 significantly enhanced oxidation rate can only be explained by the presence of an
292 actively metabolizing microbial community. This confirms that the differences in α
293 values observed between the *in situ* system and the controls can be attributed
294 to the presence of microbial activity.

295

296 3.2 Fluctuation Analysis

297 Raw and integrated profiles from a 2 Hz downsampled realization of length $n = 1000$
298 (8.3 minutes) are presented in Figure 2. The electrode response is distinct in each
299 system, as evidenced by the dramatically different random walk paths. These
300 differences would not be apparent from the slightly different potentials at which the
301 electrode stabilizes in each system (Figure 2).

302 Fluctuations and the resulting α values (scaling exponents) are plotted in Figure 3
303 for the time window for the same realization as Figure 2; the three systems exhibit
304 linear behavior from $n = 20$ to $n = 1000$, indicating a scaling range of 10 – 500 s.
305 Table 1 shows the average α value (scaling exponent) and standard error of 54
306 independent realizations (2 Hz, 5 Hz, and 10 Hz) for each of the three test systems:
307 the live system (Live; $\alpha = 1.676 \pm 0.010$); the killed system (Killed; $\alpha = 1.235 \pm$
308 0.014); and the filtered creek water system (Creek; $\alpha = 0.819 \pm 0.098$). The Live
309 system scaling exponent indicates very strong correlation; the Killed system
310 indicates moderately strong correlation, while the Creek system exhibits only
311 moderate correlation. The presence of flocculent oxides appears to induce stronger
312 correlation when compared to a fluid-only system.

313 By comparison, when the same processing steps were applied to one realization
314 from the electrode in KCl storage solution, the scaling exponent was $\alpha = 0.61$;
315 slightly higher than the expected value for a system at equilibrium, $\alpha = 0.5$,
316 indicating no correlation whatsoever (Metzler and Klafter, 2000; Jeon *et al.*, 2014).
317 This very weak correlation likely represents intrinsic instrument noise; and confirms
318 that the observed scaling exponents in the test systems result from system-intrinsic
319 correlation behaviour.

320

321 **4. Discussion**

322 *4.1 Testing of Alpha Values*

323 Two-sided t-tests on the mean α values for each system confirm that each group of
324 realizations is distinct at $p < 0.001$. Both the magnitude of drift and the shape of the
325 potential profile are common to all electrochemical techniques, and the average size
326 of a single fluctuation (as measured in step 2 of DFA) does not change over the
327 course of the measured potential. This confirms that any electrode drift is fully
328 corrected for in the detrending algorithm.

329 It must be noted that the decision to forego anti-aliasing filters comes with the
330 limitation that this particular set up is optimized for low-noise environments, or
331 those environments that can be electrically-isolated using other methods (i.e. a
332 Faraday cage) to distinguish the system of measurement from transient electrical
333 phenomena. It is also possible to include an anti-aliasing filter provided enough data
334 on the system is available to make informed decisions about rates and processes of
335 interest.

336

337 *4.2 Biogeochemical significance*

338 The ability to distinguish between different chemical solutions on the basis of
339 fluctuation behaviour presents a significant step forward in ability to monitor the *in*
340 *situ* conditions of environments of geomicrobiological significance. The variation
341 between α values indicates that biological processes give rise to stronger
342 correlation of time series measurements of fluctuations in redox potential in the
343 systems studied here. This is consistent with results of correlation analysis recently
344 reported for low biomass and high biomass circumneutral, microaerophilic Fe(II)-
345 oxidizing systems (Enright and Ferris, 2016), where the low biomass condition gave

346 rise to a scaling exponent of 1.67, and the high biomass condition gave rise to a
347 scaling exponent of 1.89 (Enright and Ferris, 2016).

348 The differences between the killed and chemical control are likely due to the
349 presence of autocatalytic Fe(II) oxidation occurring in the system with iron oxide
350 flocs. It would appear that long-range correlation in redox potential has the
351 sensitivity to distinguish different kinetic pathways *in situ*. The experimental
352 approach adopted here provides novel information about biological manipulation of
353 metabolically-significant species in solution, and about the overall chemical
354 environment a microorganism inhabits. Additionally, this technique provides a
355 means of determining whether circumneutral Fe(II) oxidation is microbially-
356 influenced or fully abiotic.

357 The dominance of a single metabolic pathway in the test site selected here
358 simplified interpretation of the observed electrochemical potentials, as the response
359 could be attributed directly to a single metabolic process: the oxidation of iron.
360 Application of this technique to other metabolic pathways and more complex
361 microbial communities may require the selection of different electrode materials, or
362 even a suite of electrodes which would make it possible to determine the behaviour
363 of individual chemical species.

364 365 *4.3 Astrobiological significance*

366 The “follow-the-energy” approach to astrobiology was first proposed in 2007
367 (Hoehler, 2007), and since that time significant progress has been made to quantify
368 minima of biological free energy (Amend and Teske, 2005; Hoehler and Jorgensen,
369 2013), and power (LaRowe and Amend, 2015a; LaRowe and Amend, 2015b).

370 However, to date, no *in situ* analysis method has been proposed to provide insight
371 into habitability as a broad concept. Due to the fact that redox potential is, in fact, a
372 measure of the chemical energy available in a system (DeLaune and Reddy, 2004),
373 there is certainly now the possibility of examining not only redox potential, but
374 the *in situ* activity of specific metabolites using ion-selective electrodes.

375 Development of this method for future missions would require consideration of the

376 detection limits of possible electrode materials, as well as their capacity to be
377 poisoned under some chemical conditions, especially in the context of hypothetical
378 metabolic pathways which could be exploited by life in these environments.

379

380 **5. Conclusion**

381 Here, we have developed a technique to distinguish biological and abiotic oxidation
382 of Fe(II) *in situ*, by quantifying RMS fluctuations of redox potential in chemical and
383 biological systems, and confirming that such fluctuation behaviour is distinct
384 between chemical and biological systems. Biological systems consistently exhibit
385 statistically significant stronger correlation behaviour than the chemical solutions
386 measured here.

387 The key benefit of this approach is its utility in field settings, and the facility of
388 comparing between niches. This technique has the potential to be applied to a wide
389 variety of environments as it requires only the possibility of placing an electrode in
390 contact with the system to be measured. We present downsampled data from a
391 system which was intentionally oversampled so as not to make any initial
392 assumptions about the nature of the interactions which might give rise to scaling,
393 however the observed scaling range necessitated downsampling data to optimize
394 realization length for the selected method. This can easily be modified to suit other
395 chemical species of interest. While iron is the only metabolite tested in here, it
396 presents a compelling case for testing additional metabolites.

397

398 **Acknowledgements**

399 This work was generously supported by a Natural Sciences and Engineering
400 Research Council of Canada (NSERC) Discovery Grant to FGF. The Ogilvies are
401 thanked for access to the field site.

402

403 **Author Disclosure Statement**

404 No competing financial interests exist.

405

406 **References**

407 Amend, J.P. and Teske, A. (2005) Expanding frontiers in deep subsurface
408 microbiology. *Palaeogeography. Palaeoclimatology. Palaeoecology* 219: 131-155.

409 Austin, W.E., and Huddleston, J.H. (1999) Visibility of permanently installed platinum
410 redox electrodes. *Soil Science Society of America Journal* 63: 1757-1762.

411 Beran, J. (1994) Statistics for long-memory processes. Chapman & Hall/CRC, New
412 York.

413 Bethke, C.M., Sanford, R.A., Kirk, M.F., Jin, Q., and Flynn, T.M. (2011) The
414 Thermodynamic Ladder in Geomicrobiology. *American Journal of Science* 311: 183-210.

415 Bibring JP, Langevin Y, Poulet F, Gendrin A, Gondet B, Berthe M, Soufflot A,
416 Drossart P, Combes M, Bellucci G and others. (2004) Perennial water ice identified
417 in the south polar cap of Mars. *Nature*, 428, 627-30.

418 Bohn, H.I. (1971) Redox potentials. *Soil Science* 112: 39-45.

419 DeLaune, D.R., and Reddy, K.R. (2004) Redox Potential. In *Encyclopedia of Soils in the*
420 *Environment* edited by D. Hillel, Academic Press, pp 366-371.

421 Dick, G.J., and Lam, P. (2015) Omics Approaches to Microbial Geochemistry.
422 *Elements*, 11, 403-408.

423 Eliazar, I.I., and Shlesinger, M.F. (2013) Fractional motions. *Physics Reports* 527: 101-
424 129.

425 Emerson, D., Fleming, E.J., and McBeth, J.M. (2010) Iron-oxidizing bacteria: an
426 environmental and genomic perspective. *Annual Reviews of Microbiology* 64: 561-583.

427 Enright, A. M. L., and F. G. Ferris (2016) Bacterial Fe(II)-oxidation Distinguished by
428 Long-Range Correlation in Redox Potential. *Journal of Geophysical Research –*
429 *Biogeosciences*, 121, doi:10.1002/2015JG003306.

430 Faulkner, S.P., Patrick W.H., and Gambrell, R.P. (1989) Field techniques for
431 measuring wetland soil parameters. *Soil Science Society of America Journal* 59: 1044-
432 1051.

433 Ferris, F.G., Enright, A.M.L., Fortin, D., and Clark, I.D. (2016) Rates of Fe(II)-
434 oxidation and Solubility of Bacteriogenic Iron Oxides. *Geomicrobiology Journal*, 33(3-
435 4): 237-242.

436 Fluhler, H., Ardakani, M.S., Stolzy, L.H. (1976) Field measured nitrous oxide
437 concentrations, redox potentials, oxygen diffusion rates, and oxygen partial
438 pressures in relation to denitrification. *Soil Science* 122: 107-114.

439 Frateur, I., Bayet, E., Keddou, M., and Tribollet, B. (1999) Local redox potential
440 measurement. *Electrochemistry Communications* 1: 336-340.

441 Gabrielli, C., Huet, F., and Keddam, M. (1993) Fluctuations in electrochemical
442 systems. II. Application to a diffusion limited redox process. *Journal of Chemical*
443 *Physics* 99: 7232- 7239.

444 Hardstone, R., Poil, S.-S., Schivone, G., Jansen, R., Nikulin, V.V., Mansvelder, H.D.,
445 and Linkenkaer-Hansen, K. (2012) Detrended fluctuation analysis: a scale-free view
446 on neuronal fluctuations. *Frontiers in Physiology* 3: 450.

447 Hoehler, T.M (2007) An Energy Balance Concept for Habitability. *Astrobiology* 7(6):
448 824-838.

449 Hoehler, T.M., and Jorgensen, B.B. (2013) Microbial life under extreme energy
450 limitation. *Nature Reviews Microbiology* 11: 83-94.

451 Hugenholtz, P. Goebel, B.M., and Pace, N.R. (1998) Impact of culture-independent
452 studies on the emerging phylogenetic view of bacterial diversity. *Journal of*
453 *Bacteriology*, 180, 4765-4774.

454 James, R.E. and Ferris, F.G. (2004) Evidence for microbial-mediated iron oxidation at
455 a neutrophilic groundwater spring. *Chemical Geology* 212: 301-311.

456 Jeon, J.-H., Chechkin, A.V., and Metzler, R. (2014) Scaled Brownian motion: a
457 paradoxical process with a time dependent diffusivity for the description of
458 anomalous diffusion. *Physical Chemistry Chemical Physics* 16: 15811.

459 Kargel JS, Kaye JZ, Head JW, Marion GM, Sassen R, Crowley JK, Prieto Ballesteros
460 O, Grant SA, and Hogenboom DL. (2000) Europa's crust and ocean: Origin,
461 composition, and the prospects for life. *Icarus*, 148, 226-265.

462 Kasem, K.K., and Jones, S. (2008). Platinum as a Reference Electrode In
463 Electrochemical Measurements. Platinum as a Reference Electrode in
464 Electrochemical Measurements. *Platinum Metals Review* 52: 100-106.

465 Kendall, B., Anbar, A.D., Kappler, A., and Konhauser, K.O. (2012) The Global Iron
466 Cycle. In *Fundamentals of Geobiology* edited by A.H. Knoll, D.E. Canfield, and K.O.
467 Konhauser, Blackwell.

468 Kim, H.-J. (2014) Anomalous diffusion induced by enhancement of memory. *Physical*
469 *Reviews E* 90: 012103.

470 LaRowe, D.E., and Amend, J.P. (2015a) Catabolic Rates, population sizes and
471 doubling/replacement times of microorganisms in the natural settings. *American*
472 *Journal of Science* 315: 167-203.

473 LaRowe, D.E., and Amend, J.P. (2015b) Power limits for microbial life. *Frontiers in*
474 *Microbiology* 6: 718.

475 Mampallil, D., Mathwig, K., Kang, S., and Leppmay, S.G. (2013) Redox couples with
476 Unequal Diffusion Coefficients: Effect on Redox Cycling. *Analytical Chemistry* 85:
477 6053-6058.

478 McSween, H.Y., Murchie, S.L., Britt, D.T., Bruckner, J., Dreibus, G., Economou, T.,
479 Ghosh, A., Golombek, M.P., Greenwood, J.P., Johnson, J.R., Moore, H.J., Parker, T.J.,
480 Rieder, R., Singer, R., and Wanke, H. (1999) Chemical, multispectral, and textural
481 constraints on the composition and origin of rocks at the Mars Pathfinder landing
482 site. *Journal of Geophysical Research* 104.

483 Metzler, R. and Klafter, J. (2000) The random walk's guide to anomalous diffusion: a
484 fractional dynamics approach. *Physics Reports* 339: 1-77.

485 Newman, D.K. and Banfield, J.F. (2002) Geomicrobiology: How Molecular-Scale
486 Interactions Underpin Biogeochemical Systems. *Science* 296: 1071-1077.

487 Ojumu, T.V., Petersen, J., and Hansford, G.S. (2008) The effect of dissolved cations
488 on microbial ferrous-iron oxidation by *Leptospirillum ferriphilum* in continuous culture.
489 *Hydrometallurgy* 94: 69-76.

490 Oldham, K.B. (1966) A Diffusion-Layer Treatment of Transient Electrochemical
491 Phenomena. *Electrochimica Acta* 11: 1475-1490.

492 Peng, C.-K., Buldyrev, S.V., Havlin, S., Simons, M., Stanley, H.E., and Goldberger, A.L.
493 (1994) Mosaic organization of DNA nucleotides. *Physical Reviews E* 49: 1685-1689.

494 Peng, C.K., Havlin, S., Stanley, H. and Goldberger, A. (1995) Quantification of scaling
495 exponents and crossover phenomena in nonstationary heartbeat time series. *Chaos*
496 5: 82-87.

497 Ramanujan, V.K., Biener, G., and Herman, B.A. (2006) Scaling behaviour in
498 mitochondrial redox fluctuations. *Biophysical Journal: Biophysical Letters* 90: L70-L72.

499 Richardson, L.F. (1926) Atmospheric Diffusion shown on a Distance-Neighbour
500 Graph. *Proceedings of the Royal Society* 110: 709.

501 Sampedro, J.A., Rosas, N., and Valdez, B. (1999) A reference electrode system for
502 electrochemical measurements at high temperature. *Corrosion Reviews* 17: 253-262.

503 Shao, Y.H., Gu, G.F., Jiang, S.Z.Q., Zhou, W.X., and Sornette, D. (2012) Comparing
504 the performance of FA, DFA, and DMA using different synthetic long-range
505 correlated time series. *Scientific Reports* 2: 835.

506 Smith, J.H., Gilbert, R.G., and Miller, J.B. (1978) Redox potential in a cropped potato
507 processing waste water disposal field with a deep water table. *Journal of*
508 *Environmental Quality* 7: 571-574.

509 Stumm, J. and Morgan, J.J. (1996) *Aquatic chemistry: chemical equilibria and rates in*
510 *natural waters*, 3rd ed.; Wiley Interscience: U.S.A.

511 Swerhone, G.D.W., Lawrence, J.R., Richards, J.G., and Hendry, M.J. (1999)
512 Construction and Testing of a Durable Platinum Ware Eh Electrode for In Situ Redox
513 Measurements in the Subsurface. *GWMMR* 132-136.

514 Taqqu, M.S., and Samorodnitsky, G. (1992) Linear models with long-range
515 dependence and finite or infinite variance. In *New directions in time series analysis*, Part
516 II, IMA Volumes in Mathematics and its Applications 46, Springer, pp 325-340.

517 van Bochove, E. Beauchemin, S., and Teriault, G. (2002) Continuous Multiple
518 Measurement of Soil Redox Potential Using Platinum Microelectrodes. *Soil Science*
519 *Society of America Journal* 66: 1813-1820.

520 Vershinin, A.V., and Rozanov, A.Gv. (1983) The Platinum Electrode as an Indicator of
521 Redox Environment in Marine Sediments. *Marine Chemistry* 14: 1-15.

522 Waite Jr JH, Lewis WS, Magee BA, Lunine JI, McKinnon WB, Glein CR, Mousis O,
523 Young DT, Brockwell T, Westlake J and others. (2009) Liquid water on Enceladus
524 from observations of ammonia and ^{40}Ar in the plume. *Nature*, 460, 487-490.

525 Weber, K.A., Achenbach, L.A., and Coates, J.A. (2006) Microorganisms pumping iron:
526 anaerobic microbial iron oxidation and reduction. *Nature Reviews Microbiology* 4: 752-
527 764.

528 Whitfield, M. (1969) Eh as an Operational Parameter in Estuarine Studies. *Limnology*
529 *and Oceanography* 14: 547-558.

530 Wiener, N.J. (1923) Differential Space. *Journal of Mathematical Physics* 2: 131-174.

531 Witt, A., and Malamud, B.D. (2013) Quantification of long-range persistence in
532 geophysical time series: conventional and benchmark-based improvement
533 techniques. *Surveys in Geophysics* 34: 541-651.

534

535 **Tables**

536

537 Table 1: The average scaling exponents (α values) and standard error (SE) of slope
538 determined for 54 realizations of time series in each of three different systems: the
539 live system (Live), and two abiotic systems: killed BIOS (Killed), and filtered creek
540 water (Creek).

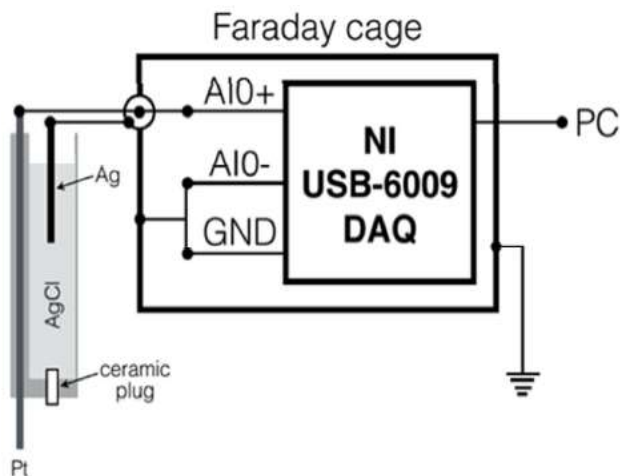
541

	Live	Killed	Creek
α	1.676	1.235	0.819
SE	0.010	0.014	0.098

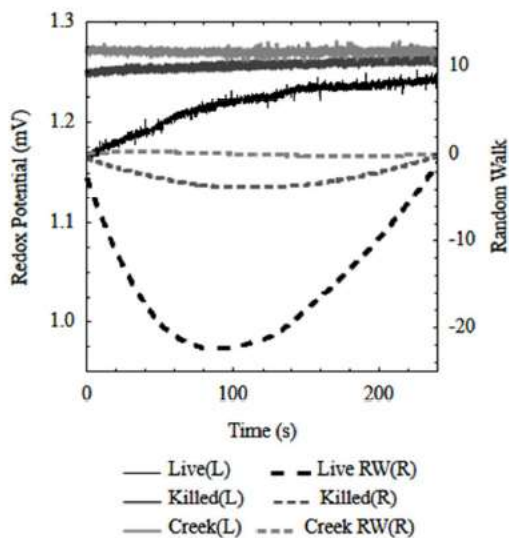
542

543

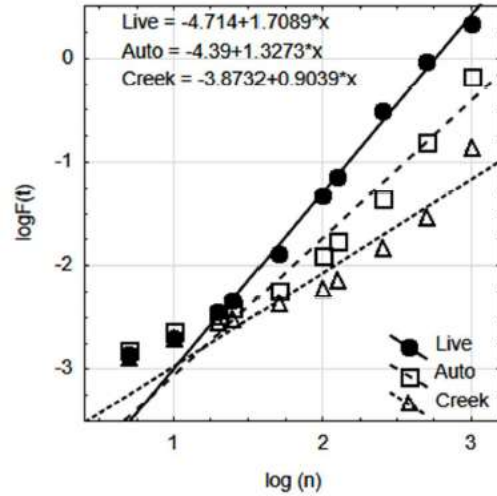
544 **Figures**
545
546



547
548
549 **Figure 1:** Schematic diagram of the experimental set up designed to measure redox
550 potential using a Pt working electrode and Ag/AgCl reference electrode. AI0+, AI0-,
551 and GND describe specific pins on the NI-6009 USB Data Acquisition Device (DAQ).
552
553
554
555



556
557
558 **Figure 2:** Oxidation-reduction potential (ORP) raw data and integrated data from
559 each of the three time series; raw data, in mV, plotted against left axis, while the
560 integrated signal is plotted on the right.



561
 562
 563
 564
 565
 566
 567
 568
 569

Figure 3: Detrended fluctuation analysis results for three experimental systems. These results represent α calculated for a single realization of each process with $n = 1000$, at measurement frequency 2 Hz. RMS is root-mean-square fluctuation as calculated using detrended fluctuation analysis (DFA). Scaling range is observed from $n = 20$ to $n = 1000$, corresponding to 10 – 500 s, short window sizes ($n = 5$, $n=10$) which do not display linearity are excluded from linear regression analysis, as outlined in description of DFA algorithm.